Band engineering of GaSbN alloy for solar fuel applications

Qing Shi,[1,*] Ying-Chih Chen,[1,†] Faqrul A. Chowdhury,[2] Zetian Mi,[2] Vincent Michaud-Rioux,[1] and Hong Guo[1]
[1]*Center for the Physics of Materials and Department of Physics, McGill University, Montréal, QC, H3A 2T8, Canada*
[2]*Department of Electrical and Computer Engineering, McGill University, Montréal, QC, H3A 0E9, Canada*

(Received 23 May 2017; published 4 August 2017)

III-nitride nanostructures possess ideal attributes for harvesting solar energy and generating solar fuel through natural water splitting. The most basic requirement of the latter is to engineer the band gap of the semiconductor to straddle the redox potential of water molecules. To this end, using first principles method we predict that GaN engineered with Sb doping at the dilute limit of 0.3% and/or slightly less is suitable for photochemical water splitting applications. The valence band edge is very significantly enhanced by dilute Sb doping while the conduction band edge is not. The microscopic physics behind the strong band bowing by such a small impurity concentration, not seen in other III-V semiconductors, is revealed by investigating the quantum interaction between Sb impurity states and the host GaN states. The dilute doping limit dictates very large systems to be calculated at the hybrid exchange-correlation level which is made possible by our newly developed first principles approach.

DOI: 10.1103/PhysRevMaterials.1.034602

I. INTRODUCTION

III-nitride material such as InGaN is one of the most important semiconductors after silicon [1–3]. Due to its exceptional optical properties, recent works have demonstrated the exciting results that III-nitride *nanostructures* possess ideal attributes for solar fuel generation through natural water splitting [4–7] and CO_2 reduction [8]. By tuning the concentration x of In, the band gap E_g of $In_xGa_{1-x}N$ can be continuously lowered from about 3.4 eV at $x = 0$ to about 0.7 eV at $x = 1$, covering broadband of the solar spectra thereby producing high solar-to-energy conversion rates [9]. For solar fuels, the nonpolar surface of InGaN can spontaneously adsorb and deform water and CO_2 molecules [8,10–12], and the nitrogen-rich surface of InGaN nanowires has the extraordinary ability of resisting photo-oxidation and corrosion in harsh photocatalytic conditions [13]. To achieve the best catalytic effects for water splitting, the band gap of the catalyst needs to properly straddle the redox potential of water molecules which is about 1.23 eV [14]. With appropriate electrochemical overpotentials at both the valence and conduction band edges, the optimal band gap is around 2.2 eV [15]. This can be achieved for InGaN by alloying high In concentration at 40% into GaN. With such concentrations, the resulting InGaN typically contains significant density of defects due to the large lattice mismatch of around 11% between InN and GaN [16–18], as well as large strain-induced polarization field [19,20]. These detrimental effects are some of the serious challenges for realizing large scale practical applications of InGaN as an advanced photo catalyst for solar fuel. It is therefore extremely important to search for other elements that can serve the same purpose as indium.

A few recent experimental investigations found that doping a small amount of antimony (Sb), at $x = 1 \sim 8\%$, the band gap of GaN was substantially reduced from 3.4 eV to about 1.9 eV at $x = 1\%$ and to about 1.5 eV at $x = 8\%$ [21–23], namely equivalent to the effect of incorporating more than 40% of indium into GaN. The most important and relevant regime for solar fuel is therefore in $0 < x < 1\%$. Clearly, such a dilute antimonide nitride provides extraordinary opportunities for band engineering, strain engineering and polarization engineering, which may well overcome the materials challenges associated with InGaN in solar fuel applications. To date, the bowing shape of band reduction of $GaSb_xN_{1-x}$ at $x < 1\%$, relevant for solar fuel application, has not been investigated either by experimental or theoretical investigations; the underlying cause for the sharp band gap reduction in the dilute Sb limit has remained unknown, and the band bending properties of GaSbN surface for the purpose of solar fuel application have not been investigated. It is the purpose of this work to understand these important issues from atomic first principles.

On the theoretical side, calculations of band gap by density functional theory (DFT) at relatively large Sb concentration [22], $x > 2\%$, found that E_g is almost saturated there. The bowing regime $0 < x < 1\%$, in which the gap of GaN is reduced to the proper value to straddle the redox potential of water, is very difficult for direct DFT analysis due to several reasons. The foremost is that simulating small x requires large supercells: For $x = 0.1\%$, at least 2000 GaN atoms must be included in the supercell to accommodate just a single Sb atom. Another difficulty is that to obtain correct E_g, higher level theories such as the hybrid exchange-correlation (XC) functional [24] are required which is computationally extremely expensive for even small supercells.

II. METHOD, RESULTS AND DISCUSSIONS

To overcome these difficulties, we have developed a powerful real space DFT method [25] with the HSE06 hybrid XC functional that accurately and efficiently predicts electronic structure of semiconductors [26] which allows us to investigate $GaSb_xN_{1-x}$ in the dilute Sb concentration limit. We found that $E_g(x)$ exhibits a sharp and continuous reduction for $x < 1\%$ and approaches a saturation for larger x. The sharp $E_g(x)$ reduction is due primarily to the appearance of Sb impurity states in the GaN gap which depends critically on

*qing.shi2@mail.mcgill.ca
†chenyc@physics.mcgill.ca

 ©2017 American Physical Society

the Sb concentration in the dilute limit. The character of the impurity states is identified from projected density of states which indicates an unusually strong interaction between the Sb atom and the nearby GaN atoms. Importantly, $E_g(x)$ of $GaSb_xN_{1-x}$ is reduced to 2.75 eV at $x = 0.175\%$ and to 2.5 eV at $x = 0.35\%$, which is the proper range to straddle the water redox potentials. This is to be compared to $In_xGa_{1-x}N$ for which In concentration needs to be $\geqslant 40\%$ to achieve the same level of gap reduction. The calculated surface band bending further confirms that E_g of GaSbN indeed straddles the redox potential of water in the dilute limit and we conclude that $GaSb_xN_{1-x}$ is well suited for solar fuel applications.

The DFT calculations were performed using the optimized norm-conserving Vanderbilt (ONCV) pseudopotentials [27] and a combined basis set of atomic orbital and plane waves [26]. Based on advanced numerical mathematics and parallelization algorithm, RESCU has extremely high efficiency in solving the Kohn-Sham DFT equation; for technical details, please refer to the original literature [25]. $7 \times 7 \times 5$ k-point mesh is used for sampling the Brillouin zone (BZ) in the self-consistent calculation of intrinsic GaN/GaSb which has a wurtzite primitive cell. The calculated supercell is scaled up according to the Sb concentration: at $x =$ 5.6, 2.7, 1.35, 0.7, 0.35, 0.175%; it contains 72, 72, 144, 288, 576, and 1152 atoms, respectively, 5.6% with two Sb atoms and all the others with one Sb atom. For low Sb concentration ($x < 0.7\%$) thus large supercell, Γ point is adequate for BZ sampling. The band gap $E_g(x)$ is correctly determined by employing the Heyd-Scuseria-Ernzerhof (HSE06) hybrid-XC functional [24,28], which predicts $E_g = 3.46$ eV for GaN and 0.55 eV for GaSb with spin-orbit coupling (SOC), in very good agreement with previous theoretical values [29,30].

For solar fuel application, the relevant compound $GaSb_xN_{1-x}$ is at the dilute limit, $0 < x \leqslant 1\%$, which has only a small lattice mismatch to GaN so that high quality materials can be readily grown [31] experimentally. As mentioned above, experimentally Sb is surprisingly efficient in reducing the GaN band gap [22,32]. At $x > 8\%$, $GaSb_xN_{1-x}$ becomes indirect band gap material. At small x, electronic property of $GaSb_xN_{1-x}$ such as $E_g(x)$ is not sensitive to the atomic arrangements so long as the Sb atoms are distributed uniformly in the material. The supercell is therefore prepared as follows. Take $x = 5.6\%$ as an example; we prepare a supercell with 72 atoms and two of the N atoms are replaced by Sb. The special quasirandom structure (SQS) technique [33] is used to confirm the accuracy of the band gap to within 0.05 eV as obtained by the chosen supercell. As mentioned above, the smallest x we investigated is 0.175% for which there are 1152 atoms inside the supercell with one Sb atom. In the dilute limit, the distance between Sb atoms is $\sim$10 Å so that little direct interaction exists between them. The atoms in the supercell are relaxed with the PBESol XC functional [34] using RESCU [25]. In the following, SOC is not considered to reduce computational cost as it only makes a difference on the band gap and electrostatic potential for less than 20 meV.

Figure 1 plots the calculated $E_g(x)$ of $GaSb_xN_{1-x}$ versus x. As x increases, $E_g(x)$ drops sharply in the range of $0 < x < 1\%$ and approaches a saturated value of about 1.8 eV for $x > 1\%$, consistent with experiment observations [22,32]. To the best of our knowledge, such a strong band bowing is unseen in other III-V materials, for instance, for $In_xGa_{1-x}N$ the E_g drops slowly with x. This distinct band bowing in Fig. 1 cannot be fit by conventional bowing formula involving a single bowing parameter b, $E_g(GaSb_xN_{1-x}) = (1-x)E_g^{GaN} + xE_g^{GaSb} - bx(1-x)$. The strong bowing in $GaSb_xN_{1-x}$ suggests strong interactions between the atoms and/or orbitals (see below). The predicted bowing in Fig. 1 is quantitatively comparable to the measured data [22]. The inset of Fig. 1 plots the calculated E_g of GaSbN and InGaN versus the relative lattice mismatch to GaN: GaSbN has a much smaller lattice mismatch than InGaN which is extremely important from a material fabrication point of view.

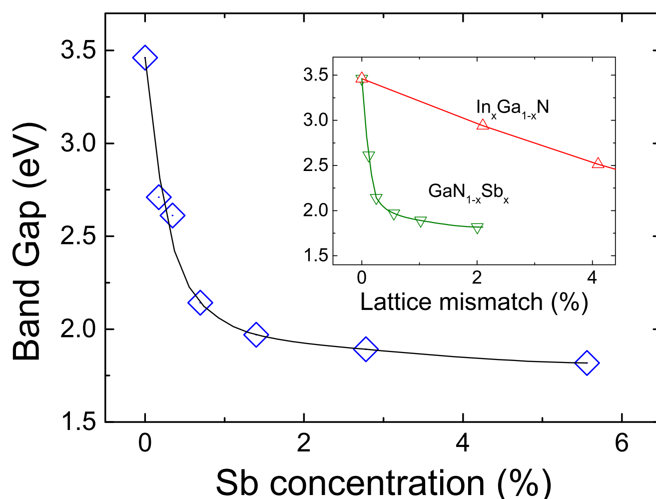

FIG. 1. Band gap $E_g(x)$ of dilute $GaSb_xN_{1-x}$ alloy vs Sb concentration x by DFT with the HSE06 hybrid functional. Inset: E_g vs lattice mismatch for $GaSb_xN_{1-x}$ (green) and $In_xGa_{1-x}N$ (red). The mismatch is measured w.r.t. wurtzite GaN crystal.

What is the microscopic origin of the strong band bowing in $GaSb_xN_{1-x}$? To interpret their experimental data, Refs. [22,32] suggested the bowing to come from the band anticrossing (BAC). Here we investigate this picture from an *ab initio* point of view by calculating the density of states (DOS) of the materials. We find that at small x, Sb atoms only contribute to the valence band (VB) of $GaSb_xN_{1-x}$ and introduce impurity states inside the GaN band gap; it has very little influence on the conduction band (CB). Therefore in Fig. 2 we plot the calculated DOS at VB side of the Fermi level, for $x = 1.35\%$, 0.35%, and 0.175%, with the curves aligned with respect to $E_{v,\mathrm{GaN}}$ which is the VB edge of GaN. We also found that VB DOS of $GaSb_xN_{1-x}$ below the zero point of the horizontal axis in Fig. 2, is very similar to that of the VB DOS of pure GaN, which means the main effect of Sb is to introduce impurity states inside the original GaN gap, namely, the sharp reduction of $E_g(x)$ and strong bowing of $GaSb_xN_{1-x}$ is due to these impurity states. As the Sb concentration x decreases, width of the impurity states becomes narrower and the main peak moves closer to $E_{v,\mathrm{GaN}}$ [see Fig. 2(a)]. This agrees reasonably well with the BAC theory [35]

$$E_\pm(k) = \frac{1}{2}\{E^v(k) + E^{Sb} \pm \sqrt{[E^{Sb} - E^v(k)]^2 + 4V^2x}\},$$

where E^v is the original GaN VB edge, E^{Sb} is the Sb impurity energy, and V the coupling parameter between impurity states

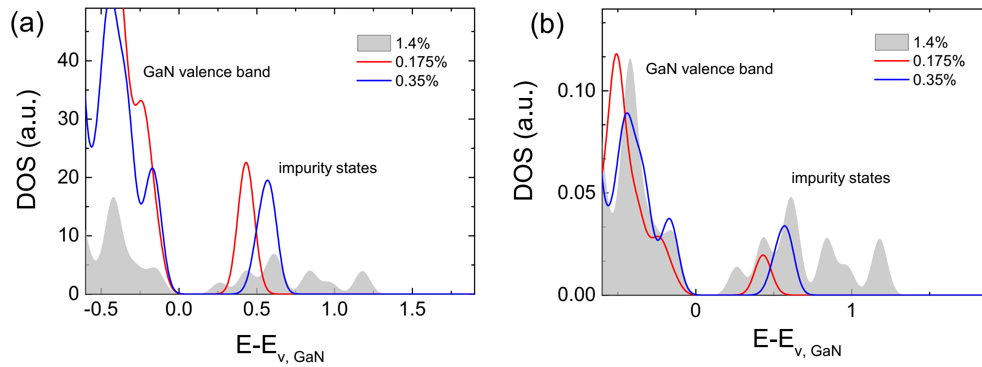

FIG. 2. DOS of $GaSb_xN_{1-x}$ at the valence band side of the Fermi level. (a) Total DOS normalized to the same number of Sb atoms at different x. The band edge of GaN, $E_{v,\mathrm{GaN}}$, is used as a reference to align the DOS at different Sb concentration. (b) Total DOS per atom. For clarity, (a), (b) do not include the calculated data at $x = 0.7\%, 2.7\%$, and 5.6% as they are similar to the presented curves of $x = 0.35\%$ and 1.4%.

and the GaN valence states. At the HSE06 level of the XC functional, $E^{Sb} \approx 0.5$ eV above the GaN VB. Then we obtain [36] $V = 6.7$ eV which is significantly larger than that of other III-V materials [35], e.g., 2.7 eV for $GaAs_xN_{1-x}$ and 3.5 eV for InP_xN_{1-x} etc.

It is also interesting to reveal how atoms interact in $GaSb_xN_{1-x}$ by projecting DOS on to each atom. At the VB edge, the p orbital of N and p,d orbital of Ga are found to dominate. For impurity states, we found the p orbital of Sb and N, as well as the p,d orbital of Ga, dominate. This indicates a strong interaction between the impurity states introduced by Sb and the GaN VB, consistent with the fitted large V parameter in the BAC model discussed in the last paragraph. As expected, it is the Ga atoms nearest neighboring to Sb that contribute to the impurity states. It is however very surprising that the p orbital of N has the largest contribution to the impurity states even though in wurzite GaSbN, the closest N atoms to Sb is only the *next* nearest neighbor. Indeed, by calculating the real space projected charge density of the impurity states, we find that Sb orbitals are mixed with those of its nearest neighbor Ga atoms and next-nearest neighbor N atoms. This can be understood by the fact that Sb has a large radius so that its orbitals can overlap and interact strongly with the next-nearest N atoms.

Having understood that the sharp reduction of $E_g(x)$ in the dilute Sb limit is due to efficient establishment of the impurity states in the GaN gap, it remains to be understood why the E_g reduction becomes very slow when $x > 1\%$, i.e., the "turning" behavior in the bowing curve Fig. 1. At large x, different Sb atoms interact with the same N atom; our investigation suggests this to weaken the interaction between Sb and N, therefore slowing down the E_g decrease. Inspecting the effective p-orbital radius of Sb and N, we find the "critical" distance between two Sb atoms to be approximately 15 Å—below which both Sb interact with the same N atom. This is very close to the average distance between Sb atoms in the case of $x = 0.7\%$, where the "turning" point is located (see Fig. 1). Another important point is the effective DOS of the impurity states: It should be comparable to that of the GaN VB to act as a "second VB." Figure 2(b) shows the total DOS per atom. We find that even at 0.175%, the DOS is on the same order as that of the GaN VB, which indeed indicates the possibility for the impurities states acting as a valence band.

Having understood the microscopic origin of the strong band bowing in the dilute Sb limit, it is extremely important to determine how bands are bent at free surfaces of $GaSb_xN_{1-x}$ for solar fuel applications. In particular, the *natural band alignment* (NBA) reflects lineup between unstrained systems which can be determined from surface calculations [9], and for solar fuel production the NBA between the semiconductor and vacuum provides useful information. For the surface calculation, we construct a repeated mirror symmetric slab supercell in the m-plane orientation $(00\bar{1}0)$ of the wurtzite $GaSb_xN_{1-x}$ structure. In this work we consider the m plane as NBA appears to be not sensitive to the crystal orientation [37]. The number of layers contained in the slab is increased until the electrostatic potential difference, ΔV, between the crystal and vacuum converges. The surface calculation allows us to align the average electrostatic potential in the crystal to the vacuum potential which acts as a common reference. Here, ΔV is calculated at the PBE level of the XC functional, and for technical details we refer interested readers to Ref. [37]. Once ΔV is obtained, the absolute positions of the band edges ($E_{c/v,\mathrm{abs}}$) with respect to the vacuum level is obtained by $E_{c,\mathrm{abs}} = E_c - \Delta V - E_0$ and $E_{v,\mathrm{abs}} = E_v - \Delta V - E_0$, where $E_{c/v}$ are the CB minimum and VB maximum of the bulk material and E_0 the average electrostatic potential of the bulk.

In the NBA calculation, structural relaxation of the slab is difficult at low Sb concentration, e.g., for $x = 0.35\%$ the slab contains about 1500 atoms. We therefore employ classical molecular dynamics to obtain the relaxed structure, by the LAMMPS method [38] with the Tersoff potential [39] found in Ref. [40]. We calibrated the potential parameters so that they produced the correct surface structures of the alloy [36]. With the relaxed structure we calculate ΔV by DFT. Figure 3 plots the calculated VB and CB alignments relative to the vacuum level. We found that surface structural relaxation tends to lower the band position by approximately 0.25 eV (not shown). This is caused by the surface dipole of the $(00\bar{1}0)$ plane of GaSbN. On the GaN $(00\bar{1}0)$ surface, Ga atoms tend to go inside the lattice so that the polar Ga-N bonds have a perpendicular component to the surface which lowers down electron affinity of GaN. In GaSbN, Sb atoms close to the surface have a similar effect according to our calculation, so that a similar reduction in band alignments is obtained. We observe that at

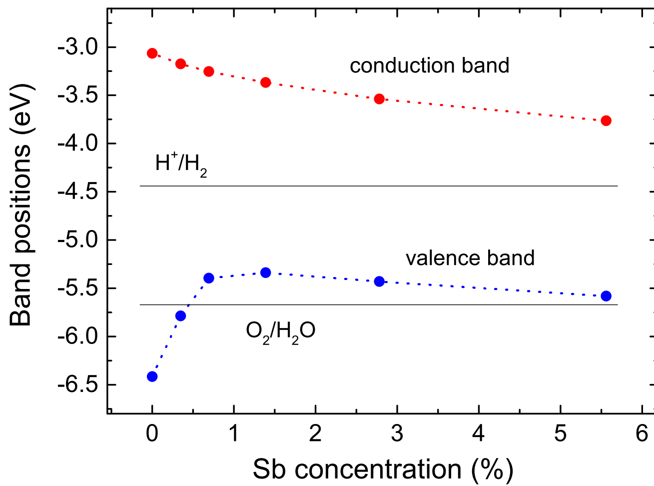

FIG. 3. Band alignments relative to the vacuum level as a function of antimony concentration x. Band positions are aligned to vacuum energy by surface calculations. The red (blue) dots/dashed line are for conduction (valence) band. Black solid lines refer to the neutral water redox potentials of H^+/H_2 and O_2/H_2O.

low Sb concentration, the VB edge varies strongly at $x < 1\%$ but approaches a saturated value beyond 1%. The CB edge varies much less. This is consistent with the finding presented above, namely impurity Sb states interact with GaN VB but not CB. Although there appears to be no simple band bowing model to describe the VB alignment as that in Ref. [9], we can find such a model to describe the CB very well. As we are only interested in the low x range $0 < x \leqslant 5.6\%$, we use the normalized concentration $x_n \equiv x/0.056$, so that,

$$E_{c,\mathrm{GaSbN}} = (1 - x_n)E_{c,\mathrm{GaN}} + x_n E_{c,5.6\%} - b x_n(1 - x_n),$$

where $E_{c,5.6\%}$ is the absolute CB edge at $x = 5.6\%$ and b the bowing parameter. Fitting the calculated data gives the bowing parameter $b = 0.62$ eV.

To achieve unassisted solar water splitting, it is essential that band edges of the semiconductor photocatalyst straddle the water redox potential which, for neutral water, is shown as the horizontal solid black lines in Fig. 3. As we can see, in order to realize neutral water splitting, Sb content must be controlled to 0.3% or slightly lower. At this doping level, the lattice mismatch is less than 0.1% which is ideal for achieving good crystal quality experimentally. Higher Sb content (>1%) may be suitable for acid water splitting.

III. SUMMARY

In summary, the band gap and band alignment of $GaSb_xN_{1-x}$ alloys are predicted for the dilute Sb limit at the HSE06 hybrid functional level. We find that the band gap decreases sharply in the Sb concentration range of $0 < x \leqslant 1\%$. The fundamental mechanism of such a sharp band bowing is found to be due to impurity states inside the band gap of GaN and a strong quantum interaction between the orbitals of Sb impurity and their surrounding neighbors and, in particular, the interaction between Sb and its next nearest neighbor N atom plays a significant role. Using the calculated natural band alignments, we predict that $x \approx 0.3\%$ and slightly lower of Sb doping should be ideal for photochemical water splitting in solar fuel applications.

ACKNOWLEDGMENTS

We gratefully acknowledge financial support of Natural Science and Engineering Research Council (NSERC) of Canada, The Fonds de recherche du Québec - Nature et technologies (FRQNT) of the Province of Quebec, and the Climate Change and Emissions Management Corporation (CCEMC) of the Province of Alberta, Canada.

[1] J. Wu, J. Appl. Phys. **106**, 011101 (2009).
[2] Y. Dong, B. Tian, T. J. Kempa, and C. M. Lieber, Nano Lett. **9**, 2183 (2009).
[3] Y. Li, J. Xiang, F. Qian, S. Gradecak, Y. Wu, H. Yan, D. A. Blom, and C. M. Lieber, Nano Lett. **6**, 1468 (2006).
[4] K. Maeda, K. Teramura, D. Lu, T. Takata, N. Saito, Y. Inoue, and K. Domen, Nature (London) **440**, 295 (2006).
[5] S. Fan, B. AlOtaibi, S. Y. Woo, Y. Wang, G. A. Botton, and Z. Mi, Nano Lett. **15**, 2721 (2015).
[6] B. AlOtaibi, H. Nguyen, S. Zhao, M. Kibria, S. Fan, and Z. Mi, Nano Lett. **13**, 4356 (2013).
[7] C. Liu, J. Tang, H. M. Chen, B. Liu, and P. Yang, Nano Lett. **13**, 2989 (2013).
[8] B. AlOtaibi, S. Fan, D. Wang, J. Ye, and Z. Mi, ACS Catalysis **5**, 5342 (2015).
[9] P. G. Moses and C. G. Van de Walle, Appl. Phys. Lett. **96**, 021908 (2010).
[10] B. AlOtaibi, X. Kong, S. Vanka, S. Y.-M. Woo, A. Pofelski, F. Oudjedi, S. Fan, M. G. Kibria, G. A. Botton, W. Ji *et al.*, ACS Energy Lett. **1**, 246 (2016).
[11] S. Zhao, H. P. Nguyen, M. G. Kibria, and Z. Mi, Prog. Quantum Electron. **44**, 14 (2015).
[12] M. Kibria, S. Zhao, F. Chowdhury, Q. Wang, H. Nguyen, M. Trudeau, H. Guo, and Z. Mi, Nature Commun. **5**, 3825 (2014).
[13] M. G. Kibria, R. Qiao, W. Yang, I. Boukahil, X. Kong, F. A. Chowdhury, M. L. Trudeau, W. Ji, H. Guo, F. Himpsel *et al.*, Adv. Mater. **28**, 8388 (2016).
[14] S. Trasatti, Pure Appl. Chem. **58**, 955 (1986).
[15] M. G. Walter, E. L. Warren, J. R. McKone, S. W. Boettcher, Q. Mi, E. A. Santori, and N. S. Lewis, Chem. Rev. **110**, 6446 (2010).
[16] S. Strite and H. Morkoç, J. Vac. Sci. Technol. B **10**, 1237 (1992).
[17] K. Kim, W. R. L. Lambrecht, and B. Segall, Phys. Rev. B **53**, 16310 (1996).
[18] A. Wright, J. Appl. Phys. **82**, 2833 (1997).

[19] F. Bernardini and V. Fiorentini, Phys. Stat. Sol. (b) **216**, 391 (1999).
[20] A. Romanov, T. Baker, S. Nakamura, and J. Speck, J. Appl. Phys. **100**, 023522 (2006).
[21] K. Yu, W. Sarney, S. Novikov, D. Detert, R. Zhao, J. Denlinger, S. Svensson, O. Dubon, W. Walukiewicz, and C. Foxon, Appl. Phys. Lett. **102**, 102104 (2013).
[22] S. Sunkara, V. K. Vendra, J. B. Jasinski, T. Deutsch, A. N. Andriotis, K. Rajan, M. Menon, and M. Sunkara, Adv. Mater. **26**, 2878 (2014).
[23] R. M. Sheetz, E. Richter, A. N. Andriotis, S. Lisenkov, C. Pendyala, M. K. Sunkara, and M. Menon, Phys. Rev. B **84**, 075304 (2011).
[24] J. Heyd, G. E. Scuseria, and M. Ernzerhof, J. Chem. Phys. **118**, 8207 (2003).
[25] V. Michaud-Rioux, L. Zhang, and H. Guo, J. Comput. Phys. **307**, 593 (2016).
[26] Y.-C. Chen, J.-Z. Chen, V. Michaud-Rioux, and H. Guo, McGill University (2017).
[27] D. R. Hamann, Phys. Rev. B **88**, 085117 (2013).
[28] In the HSE06 calculation, the standard mixing parameter $\alpha = 0.25$ and range separation parameter $\mu = 0.2$ were used.
[29] I. Vurgaftman and J. Meyer, J. Appl. Phys. **94**, 3675 (2003).
[30] A. De and C. E. Pryor, Phys. Rev. B **81**, 155210 (2010).
[31] M. Kibria, F. Chowdhury, S. Zhao, B. AlOtaibi, M. Trudeau, H. Guo, and Z. Mi, Nat. Commun. **6**, 6797 (2015).
[32] N. Segercrantz, K. Yu, M. Ting, W. Sarney, S. Svensson, S. Novikov, C. Foxon, and W. Walukiewicz, Appl. Phys. Lett. **107**, 142104 (2015).
[33] A. Zunger, S. H. Wei, L. G. Ferreira, and J. E. Bernard, Phys. Rev. Lett. **65**, 353 (1990).
[34] J. P. Perdew, A. Ruzsinszky, G. I. Csonka, O. A. Vydrov, G. E. Scuseria, L. A. Constantin, X. Zhou, and K. Burke, Phys. Rev. Lett. **100**, 136406 (2008).
[35] J. Wu, W. Shan, and W. Walukiewicz, Semicond. Sci. Technol. **17**, 860 (2002).
[36] See Supplemental Material at http://link.aps.org/supplemental/10.1103/PhysRevMaterials.1.034602 for further details on some of the issues in the paper. Section I provides detailed information on how the coupling parameter V is obtained. Section II lists the parameters used in the molecular dynamics simulation.
[37] A. Franciosi and C. G. Van de Walle, Surf. Sci. Rep. **25**, 1 (1996).
[38] S. Plimpton, J. Comput. Phys. **117**, 1 (1995).
[39] J. Tersoff, Phys. Rev. B **39**, 5566 (1989).
[40] D. Powell, M. A. Migliorato, and A. G. Cullis, Phys. Rev. B **75**, 115202 (2007).